Contribution from the Laboratorio di Chimica Quantistica ed Energetica Molecolare, CNR, 56100 Pisa, Italy, and the Laboratorio di Teoria e Struttura Elettronica dei Composti di Coordinazione, CNR, Rome, Italy

Charge Effects on the Radiative Decay of X-Ray Ions. Model Calculations for Some Transition Metals

F. A. GIANTURCO,* E. SEMPRINI, and F. STEFANI

Received May 16, 1975 AIC503428

The effect of perturbed valence-shell populations on the energies associated with radiative decays following X-ray ionization is examined and the relevant shifts are computed within the "free ion" model for the transition metal series. The different terms contributing to the emitted photon energies are examined for $K\alpha_{1,2}$, $K\beta_{1,3}$, $K\beta_5$, and LM fluorescence lines and their relative importance is discussed. The different trends in "chemical" shifts exhibited by the $K\alpha_{1,2}$ and other emission channels when varying the number of 3d and 4s electrons in the valence shells are computed and explained within the framework of simplified, local interaction potentials.

1. Introduction

Extensive theoretical and experimental effort has been expended to calculate and measure single-particle binding energies in many-body systems.[1]

If a particle is removed, it is evident that the remaining particles are affected and will generally respond with some sort of rearrangement. This rearrangement contributes to the energy needed to remove a particle and must be considered in comparisons between experiment and theory.[2,3]

Physical intuition suggests that if a particle is removed suddenly (vanishes instantly from the original system) or, on the other hand, adiabatically (i.e., is dragged out very slowly), the remaining particles will respond differently.

This is the qualitative basis for the concept of a relaxation or rearrangement time of the systems: the time required for a collective response to removal. In a sudden removal the system will be strongly perturbed and in quantum mechanical terms other particles will be "shaken" into excited bound states or into continuum states.[4]

Since one can assume that there is no time to rearrange, it has been previously suggested that a "frozen-orbital" picture applies to such situations.[5] In the other limit, however, the particle moves away with little energy above threshold and the remaining system adjusts at each stage: according to the time evolution and the spectral structure of the target system shaking can thus be made arbitrarily small.[6] Therefore the maximum extra energy that a particle can pick up in a slow removal is the difference between the single-particle eigenvalue in the Hartree–Fock (HF) scheme for a closed-shell configuration and the lowest peak in the photoionization spectra of the molecular targets.

The reference level in electron binding energy calculations is generally chosen as the vacuum level.[1] The electron binding energy, $(BE)_K$, is then by definition the least energy required to extract the electron from the system to infinity. This obviously implies that

$$(BE)_K = E^\circ(N-1, K) - E^\circ(N) \quad (1)$$

where $E^0(N-1, K)$ and $E^\circ(N)$ are the lowest eigenvalues for the $\mathcal{H}(N-1, K)$ and $\mathcal{H}(N)$ Hamiltonians, respectively. Via the standard definitions of effective Hamiltonians[7] one can then rewrite eq 1 as given by various contributions

$$(BE)_K = E^\circ_{HF}(N-1, K) - E^\circ_{HF}(N) + \delta E^{cor} + \delta E^{relat} \quad (2)$$

the last two terms on the right-hand side being the differences of the correlation and relativistic energies of the final and initial states, respectively. In the "frozen-orbital" situation one can further modify the above equality by invoking the well-known Koopmans theorem result[5] and making use of the Lagrange multiplier for the relevant orbital K, ϵ_K^{HF}

$$(BE)_K = -\epsilon_K^{HF} + E_K^{relax} + \delta E_K^{cor} + \delta E_K^{relat} \quad (3)$$

E_K^{relax} is now the relaxation energy (negative) for the infinitely adiabatic process, which always appears as the strongest contribution to photoionization curves over large energy ranges.[4] This term is seen to be substantial for core electrons of even the lightest atoms, whereas it appears to be at least an order of magnitude smaller for outer electrons in both atoms and molecules.[8] Moreover, the contributions to eq 3 of only the first two terms yield binding energies smaller than the experimental ones, in agreement with what one expects, viz., that the total correlation energy should be somewhat larger for the initial N-electron system than for the final $(N-1)$-electron configuration.[9] Their use becomes therefore a sound one only when the ionized shell exhibits very small intrashell correlation contributions, terms usually considered to be the most important.

Finally, although the relativistic corrections can also be found to be appreciable even for light atoms, they are markedly altering the agreement with experiments for $Z \approx 20$ onward and mainly for the inner shells, as we shall see in the following section.

Whenever the target molecule (or atom) decays radiatively, however, the observation of its fluorescence lines in the X-ray energy region can be compared with computed estimates that essentially use the *differences* between the values of eq 3, thus greatly reducing the contributions to $(BE)_K$ from most of the terms on the right-hand side of the above equation.[5]

Even the "frozen-orbital" picture yields therefore reasonably good agreement with measured lines and obviously reduces the computational effort to having only to produce reliable ground-state descriptions of the HF wave functions.[8] Moreover, the wealth of lines presented by systems like the transition metals could be an interesting field of comparison for analyzing the *differential* effects of ionization on the various levels involved in the fluorescence transitions.

That such transitions exhibit energy shifts along series of chemical compounds has been recognized long ago[10] and found to be qualitatively well reproduced by "free-ion" model calculations.[5,11,12] In the present work we extend the above model to transition metals with the aim of assessing in some systematic way the charge effects over a variety of radiative decay channels involving different types of inner electrons. The relevant fluorescence line energies are presented in section 2 together with the different shifts generated by 3d- or 4s-orbital removals.

The possible generalizations and comparison of effects over a given range of Z values are then discussed in section 3.

2. The Computational Model

(a) Kα, Kβ, and LM Fluorescence Lines. As mentioned above, the highly excited ions produced by removal of a core electron quickly decay by photon emission, this being in

* To whom correspondence should be addressed at the Istituto di Chimica Fisica, Pisa, Italy.

Table I. Computed Fluorescence Line Energies from Inner Shells of Transition Metal Atoms[a]

	Ti	V	Cr	Mn	Fe	Co	Ni	Cu
$K\alpha_{1,2}$ b	4502.7	4938.1	5394.3	5869.8	6366.0	6882.6	7419.5	7977.3
$K\alpha_{1,2}$ c	4502.7	4938.0	5394.2	5869.7	6366.0	6882.6	7419.5	7977.3
$K\alpha_{1,2}$ d	4508.8	4949.7	5411.1	5894.4	6399.5	6925.3	7472.4	8041.1
$K\beta_{1,3}$ b	4938.0	5427.9	5940.9	6477.5	7037.4	7620.4	8226.7	8855.9
$K\beta_{1,3}$ c	4938.1	5428.1	5941.1	6477.8	7037.5	7620.6	8226.7	8855.9
$K\beta_{1,3}$ d	4931.8	5427.3	5946.7	6490.5	7058.0	7649.4	8264.7	8905.03
$K\beta_5$ b	4974.8	5469.0	5986.5	6527.5	7094.4	7683.8	8296.6	8933.1
$K\beta_5$ c	4976.1	5470.7	5989.1	6530.6	7096.0	7684.8	8297.1	8933.0
$K\beta_5$ d	4962.3	5462.9	5986.9	6535.2	7108.1	7705.9	8328.6	8977.0
$L_IM_{II,III}$ b	534.1	594.7	657.4	724.6	794.3	867.0	942.6	1020.2
$L_IM_{II,III}$ c	534.2	594.9	657.7	725.1	794.6	867.1	942.6	1020.2
$L_IM_{II,III}$ d		585.0	654.0	721.0	792.0	870	941	1022.8
$L_{II}M_I$ b	405.9	458.2	513.0	571.3	632.5	696.5	763.3	832.8
$L_{II}M_I$ c	406.0	458.3	513.3	571.7	632.7	696.6	763.4	832.8
$L_{II}M_I$ d	401.3	453.5	510.2	567.5	628.0	694.0	762.0	832.0

[a] See text for meaning of symbols; values in eV units. [b] From ref 17. [c] Present work. [d] Experimental values.[13]

competition with a wide variety of alternative channels of a nonradiative nature (Auger electrons, etc.).[4] The energy balance for the primary process can then be written simply as

$$E_{[K]} = E_{[L]} + E_{K\alpha}{}^{h\nu} \tag{4}$$

where the total electronic energies (in the Born–Oppenheimer sense, for molecules) of the $(N-1)$-particle systems are labeled with the shell carrying the vacancy written in brackets and the photon energy corresponds to eq 4 to the $K\alpha$ fluorescence line. The traditional nomenclature also establishes that $K\beta$ lines are associated with final vacancies in the M shell whereas initial holes in the 2s and 2p orbitals would correspond to LM lines for the transition metal series.[13]

According to eq 3 we can therefore write for the photon energy of eq 4

$$E_{K\alpha}{}^{h\nu} = (\epsilon_L{}^{HF} - \epsilon_K{}^{HF}) + (E_K{}^{relax} - E_L{}^{relax}) + (\delta E_K{}^{relax} - \delta E_L{}^{relax}) + (\delta E_K{}^{cor} - \delta E_L{}^{cor}) \tag{5}$$

hence

$$E_{K\alpha}{}^{h\nu} = \Delta\epsilon_K{}^{HF} + \Delta E_{K\alpha}{}^{relax} + \Delta E_{K\alpha}{}^{relat} + \Delta E_{K\alpha}{}^{cor} \tag{6}$$

One can then try to estimate the relative contributions of the four terms in eq 6 in order to establish some priorities in "escalating" computational accuracy.[8] Since both initial and final states have the same number of electrons, it is reasonable to expect that differences of correlation corrections can be disregarded for radiative decay;[9] hence

$$E_{K\alpha}{}^{h\nu} \simeq \Delta\epsilon_K{}^{HF} + [\Delta E_{K\alpha}{}^{relax} + \Delta E_{K\alpha}{}^{relat}] \tag{7}$$

The two terms within brackets on the right-hand side of (7) have opposite signs, since relaxation corrections are stabilizing the systems,[14] whereas neglect of relativity tends to give estimates of binding energies that are too small when compared with experiments.[15] It is also known that relativistic effects are most important for large binding energies, as the electron's velocity in the relevant bound state is no longer negligible when compared to the velocity of light. The necessary correction thus increases the electron kinetic energy; hence the total binding energy decreases.

It therefore follows that the interplay of the above two terms will be reflected on the found agreements between experimental data and the "frozen-orbital" energy values, i.e., the first term only of eq 7. In fact for light atoms or for outer electrons the relevant ΔE^{relat} are usually negligible or anyway smaller than relaxation effects. The $\Delta\epsilon^{HF}$ will therefore overestimate the energies for fluorescence lines. For inner electrons of heavy atoms the opposite is usually true; hence $\Delta\epsilon^{HF}$ will be smaller than experimental $E^{h\nu}$ values. In either case, however, the net corrections are very small and the use of Koopmans theorem reproduces the experimental data[5,12] remarkably well.

We have computed such energies for the atom series from V to Cu, with variational solutions of the HF equations after expansions over rather extended sets of analytic functions (STO's). Either the multiplets originating from the outer shells were averaged in order to yield average energies for each atom,[16] or the lowest energy components were chosen as reference configurations.[17] The results are presented in Table I where a comparison is also made with the experimental findings available in the literature.[13]

The competing effects discussed before are clearly displayed for the $K\alpha_{1,2}$ lines along the whole series: relativistic corrections of the order of $\sim 10^2$ eV for K-shell electrons[15] are outbalancing the lack of relaxation effects in the $\Delta\epsilon^{HF}$'s, thus giving increasingly smaller computed values. For the [K] → [M] transitions the effect is reversed by the increased ΔE^{relax} values, this being even more so when only outer electrons are involved, as in the [L] → [M] processes, where the relativistic effect is drastically reduced. In almost all cases however the computed values fall within 1% of the experiments, thus confirming the fairly satisfactory performance of simply sudden models for such radiative processes.

Transition metal complexes usually display a rich electronic absorption spectrum in the visible and near-uv regions, since there are several possibilities for outer excitations, the ligand-field and charge-transfer excitations being the most commonly quoted.[18] This is one of the consequences of the perturbed electronic structure of the central metal, where competitive polarization exists between outer 3d and 4s functions. The fluorescence spectra should also reflect such a situation and be differently affected in terms of energy and line shapes along series of compounds.

A possible model approach is therefore presented below and discussed in section 3.

(b) Fluorescence Transitions between Multiple Ions. The electronic rearrangement occurring as chemical bonds are formed can be pictorially explained by attributing what is called an effective charge q to the atom in the compounds as compared with the neutral, free atom. Obviously for an exact definition of q it is necessary to find some criteria for the allocation of valence electrons, and several "experimental" methods have been suggested over the years, starting from a wide variety of spectroscopic techniques involving outer electrons.[19] Since however core electrons do not take active part in the bonding, the interpretation of molecular data involving such electrons has often strived for the definition of effective, local potentials that could describe the bonding effects in a simple form[5,14,20] and could also account for the energy shifts exhibited by emitted electrons and photons from inner molecular levels.

Table II. Computed Energy Shifts (eV) for Inner-Shell Fluorescence Lines in Transition Metal Ions

	Ti^+ $3d^14s^2$, ^2D	V^+ $3d^24s^2$, ^3F	Cr^+ [b] $3d^34s^2$, ^4F	Mn^+ $3d^44s^2$, ^5D	Fe^+ $3d^54s^2$, ^6S	Co^+ $3d^64s^2$, ^5D	Ni^+ $3d^74s^2$, ^4F
$\delta(K\alpha_{1,2})$	−0.784	−0.766	−0.734	−0.741	−0.646	−0.633	−0.642
$\delta(K\beta_{1,3})$	0.910	0.906	0.918	0.983	0.683	0.785	0.776
$\delta(K\beta_5)$	1.685	0.864	0.642	1.158	−1.534	−0.491	−0.294
$\delta(L_IM_{II,III})$	1.841	1.818	1.795	1.870	1.463	1.552	1.553
$\delta(L_{II}M_I)$	1.089	1.087	1.079	1.149	0.812	0.899	0.904

[a] Missing 3d; see text. [b] The zero-point configuration is given by [$3d^44s^2$, ^5D] whereas all the others are given by neutral-atom ground states (see Table I).

Table III. Computed Energy Shifts (eV) for Inner-Shell Fluorescence Lines of Transition Metal Negative Ions[a]

	Ti^- $3d^34s^2$, ^4F	V^- $3d^44s^2$, ^5d	Cr^- [b] $3d^54s^2$, ^6S	Mn^- $3d^64s^2$, ^5D	Fe^- $3d^74s^2$, ^4F	Co^- $3d^84s^2$, ^3F	Ni^- $3d^94s^2$, ^2D
$\delta(K\alpha_{1,2})$	0.527	0.527	0.584	0.465	0.477	0.516	0.499
$\delta(K\beta_{1,3})$	−0.124	−0.162	−0.207	0.017	−0.112	−0.097	−0.147
$\delta(K\beta_5)$	0.172	0.246	−0.259	2.094	1.105	0.932	0.747
$\delta(L_IM_{II,III})$	−0.761	−0.802	−0.914	−0.554	−0.699	−0.727	−0.763
$\delta(L_{II}M_I)$	−0.224	−0.255	−0.341	−0.053	−0.178	−0.199	−0.227

[a] Added 3d; see text. [b] The zero-point configuration is here [$3d^44s^2$, ^5D].

Table IV. Computed Energy Shifts (eV) for Inner-Shell Fluorescence Lines in Transition Metals[a]

	Ti^+ $3d^24s^1$, ^4F	V^+ $3d^34s^1$, ^5F	Cr^+ $3d^54s^0$, ^6S	Mn^+ $3d^54s^1$, ^7S	Fe^+ $3d^64s^1$, ^6D	Co^+ [b] $3d^84s^0$, ^3F	Ni^+ [b] $3d^94s^0$, ^2D	Cu^+ $3d^{10}4s^0$, ^1S
$\delta(K\alpha_{1,2})$	0.050	0.037	0.157	0.043	0.058	0.121	0.132	0.112
$\delta(K\beta_{1,3})$	0.105	0.085	−0.068	0.096	0.071	−0.041	−0.047	−0.053
$\delta(K\beta_5)$	−0.007	−0.017	−0.202	0.008	0.003	0.034	−0.096	−0.099
$\delta(L_IM_{II,III})$	0.029	0.023	−0.279	0.025	−0.014	−0.207	−0.227	−0.208
$\delta(L_{II}M_I)$	0.103	0.095	−0.084	0.099	0.071	−0.051	−0.068	−0.060

[a] The ions shown refer to a missing 4s electron; the shifts are referred to neutral species. [b] The zero-point configurations are [$3d^84s^1$, ^4F] and [$3d^94s^1$, ^3D] for Co and Ni, respectively. The other reference configurations are the ones of Table I.

The direct evaluation of such chemical shifts from completely "ab initio" computed wave functions, although greatly extended in recent years by the more general availability of MO–LCAO computer codes,[8] still presents conceptual problems and involves sizable amounts of computation.

The "free-ion" model employs instead calculations of free ions and atoms and attributes the radiative channel wavelength of an atom A in a compound to the one of a corresponding ion with definite charge, to which the effective charge of the relevant "atom" in the compound should then correspond. Since the electroneutrality conditions—i.e., that $q_A = -\sum_{B_i \neq A} {}^nq_{B_i}$ with the B_i's being the other molecular "atoms" in the examined compound—are usually satisfied in such experiments, one obviously expects to overestimate electron energy shifts but to get very close to the experimental photon energy shifts where *differential* effects are sampled.

Calculations have therefore been performed for transition metals in order to compare the different effects of ionizing 3d or 3s electrons on the shifts presented by a given fluorescence line J

$$\delta E_J{}^{h\nu} = (E_J{}^{h\nu})_{ion} - (E_J{}^{h\nu})_{atom} \quad (8)$$

Table II presents the results for positive ions with one 3d electron missing. The calculations were performed by using the lowest spectral term of each configuration and referring them to the neutral configurations of Table I. The basis set expansions were the ones recently reported in the literature.[17] Computations were also done for the corresponding average configurations[21] which provide a monocentric description of the random spin distributions generated by bond formation.[12] The corresponding effect of negative charge migration is described by the results of Table III, where negative ion configurations are reported with an added 3d electron and where the expected electrostatic effect that changes sign to the shifts is exhibited by the lines. In all the above cases the differences are taken from the neutral, ground-state configurations of Table I unless otherwise stated in each specific table.

Table V. Computed Energy Shifts (eV) for Different Ionic States of Ti and V[a]

	Ti		V		
	1+	2+	1+	2+	3+
$\delta(K\alpha_{1,2})$	−0.756	−1.709	−0.729	−1.601	−2.640
$\delta(K\beta_{1,3})$	−0.838	2.656	0.860	2.664	5.495
$\delta(L_IM_{II,III})$	1.736	4.678	1.729	4.593	8.609
$\delta(L_{II}M_I)$	1.010	3.075	1.023	3.024	6.157

[a] Both parent and daughter species are given by averaged configurations.

Table IV collects the positive ion shifts, when an electron is removed from the 4s subshell, for all the fluorescence lines reported before: the magnitude of such shifts is clearly much smaller than for the 3d-electron removal and it remains so for the whole group of lines.

Finally, a series of ions with multiple vacancies in the outer shells was computed for vanadium and titanium with random spin distributions within such shells and the results are reported in Table V. Although little physical significance should be attached to, say, V^{3+} configurations in molecules, the charge dependence is however provided in order better to establish "calibration" curves. Such curves can in turn provide, from experimental shifts, the expected values for effective charges[22] on the host atom. Figure 1 reports such curves for V and Ti ions and for all the fluorescence lines involving inner shells. The negative ions were those computed before via spectroscopic terms, but very little difference was found between them and the averaged energies for neutrals and positive ions reported in Table V.

3. Discussion of Results

The search for effective potentials generated by inner electrons in molecular systems and generally felt between "far away" shells is based usually on the assumption that, according

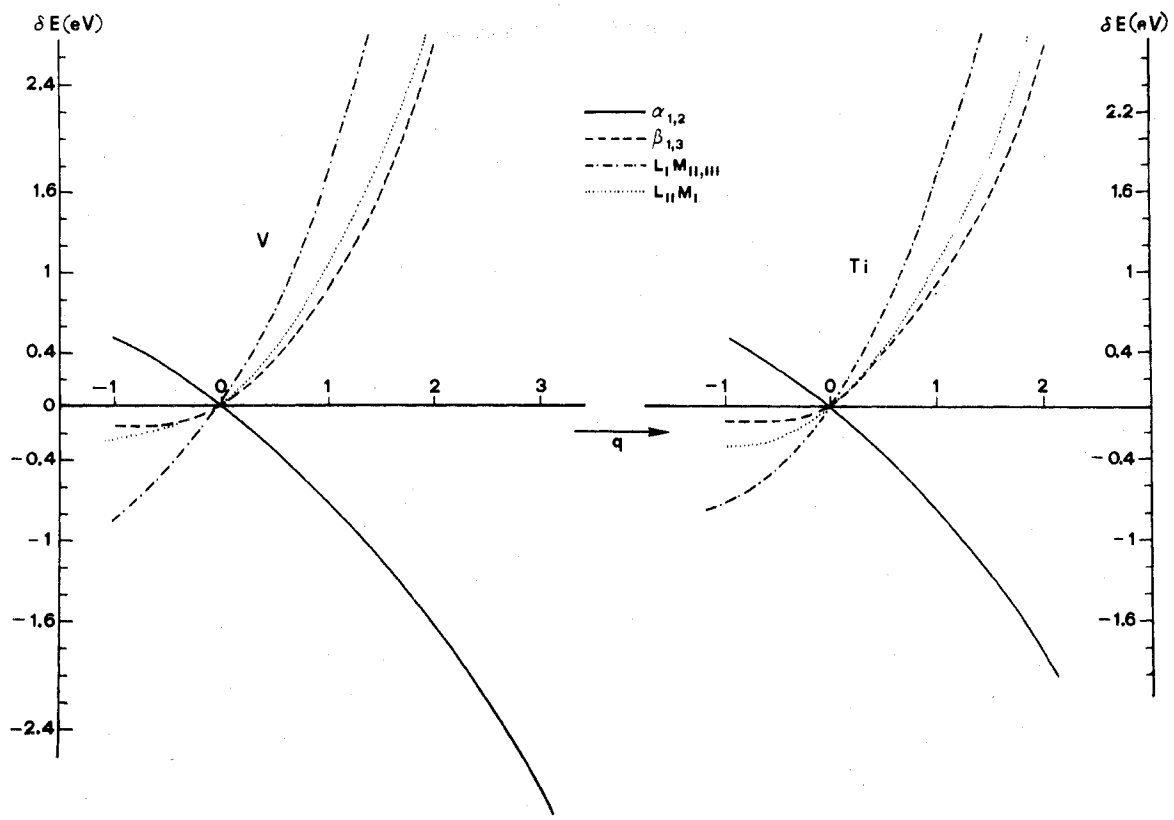

Figure 1. Fluorescence line energy shifts (in eV) vs. effective charges q of the valence shells in vanadium (left) and titanium (right). The energies reported for each computed line refer to the weighted average of the LS multiplets.

Table VI. Calculated $\langle r_{nl} \rangle$ Values (in au) for Some Orbitals of Average Configuration of Neutral Transition Metals

	Ti ($3d^2$)	V ($3d^3$)	Cr ($3d^4$)	Mn ($3d^5$)	Fe ($3d^6$)	Co ($3d^7$)	Ni ($3d^8$)	Cu ($3d^9$)
$\langle r_{1s} \rangle$	0.070116	0.067000	0.064147	0.061527	0.059112	0.056878	0.054807	0.052881
$\langle r_{2p} \rangle$	0.289586	0.274032	0.260092	0.247531	0.236132	0.225754	0.216262	0.207547
$\langle r_{3p} \rangle$	1.093773	1.025161	0.965628	0.913717	0.865865	0.823553	0.785477	0.751009
$\langle r_{4s} \rangle$	3.778717	3.626237	3.493746	3.381895	3.258444	3.153545	3.059060	2.973317
$\langle r_{3d} \rangle$	1.459781	1.323240	1.219249	1.130063	1.072738	1.016049	0.964705	0.918262

to Unsold's theorem, the charge distributions due to filled subshells are rigorously spherically symmetrical about the nucleus; hence the effect felt "outside" such subshells is as though it were generated by point charges concentrated at the relevant nucleus.[14]

If this model is combined with the now well-known fact that the shape of a core electron is affected little by valence charge redistribution,[23] the average energy of interaction between an inner orbital ϕ_i and an outer, valence orbital ϕ_v will then change little along a series of ions of the same atom and should approximately[24] be given by the relevant nuclear repulsion integrals for the orbital ϕ_v, viz., $\langle \phi_v | r^{-1} | \phi_v \rangle$. The population changes of such outer shells will therefore be the main factors in the energy shifts observed in core electron spectra, shifts that will be nearly constant for any of such inner orbitals and that often exhibit a linear charge energy relationship[25] along series of compounds.

The fluorescence line shifts, on the other hand, are a suitable test for the validity range of such an approximate model, since their sampling of differential effects will be possible just because physical reality departs from point charge behavior.

The lack of complete shielding by outer shells of the inner electrons does, in fact, show up when correct HF computations are performed and accounts for the differences in energy shifts observed when 1s or 2p electrons are involved in, for example, sulfur compound emission lines.[11,12]

The series of lines computed here for transition metals clearly exhibit such behavior, as already reported by the tables discussed in the previous section, but their more complex structure also allows one to make some estimates as to how well their valence electrons fit the model of a point charge interaction. The removal of a 4s electron, for instance, shows very small "chemical" shifts along the whole series of metals examined. A look at their computed $\langle r \rangle$ values with respect to those for inner orbitals (Table VI) suggests in fact that the corresponding $\langle r^{-1} \rangle_{4s}$ values would provide a rather good approximation to their interactions with 1s and 2s and with 2p and 3p electrons,[24] thus fitting the effective-interaction model for K, L, and M shells. It follows then that the relative changes in screening upon 4s removal will be almost the same for those shells and therefore very small shifts will be observed for the Kα and Kβ fluorescence lines.

This is not the case for 3d electrons, which penetrate more deeply into the core region and therefore exhibit much more noticeable differential screening effects between the levels relevant to the various fluorescence lines. As one sees from the tables all the computed shifts are, in fact, larger than in the previous case and exhibit the relative signs already found for the elements of the previous row in the periodic table,[5,12,16] where 3s and 3p valence electrons were involved, i.e., positive for cations and negative for anions.

For the K$\alpha_{1,2}$, however, the electrostatic picture is still largely preserved, since the 3d screening is very similar for both K and $L_{II,III}$ subshells. A reduction (or increase) of the 3d-orbital population will however stabilize (or destabilize) 2p-hole states *less* than 1s-hole states because the radial charge

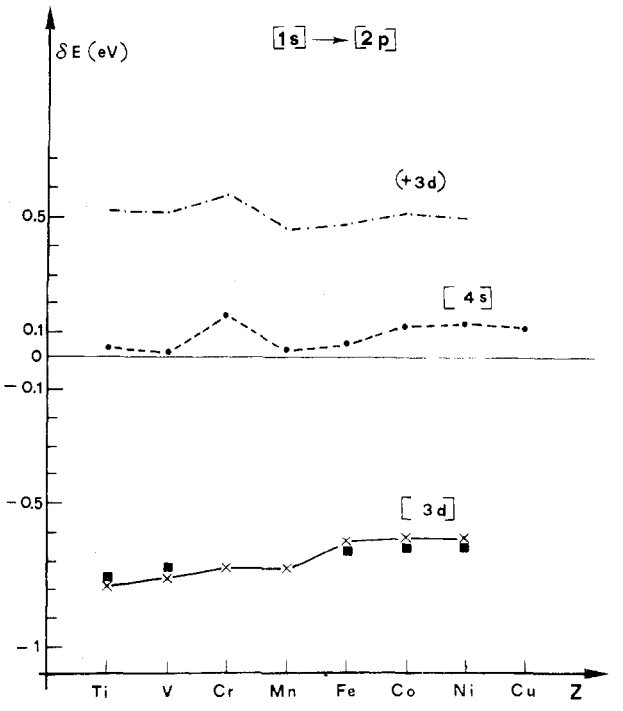

Figure 2. "Chemical" shifts for $K\alpha_{1,2}$ fluorescence lines as a function of the atomic number Z and for varying outer-shell populations: X–X–X, [3d], one vacancy in the 3d subshell; •- - - -•, [4s], one vacancy in the 4s subshell; - · - · -, (+3d), one electron added in the 3d subshell; ■ ■, average energy calculations.

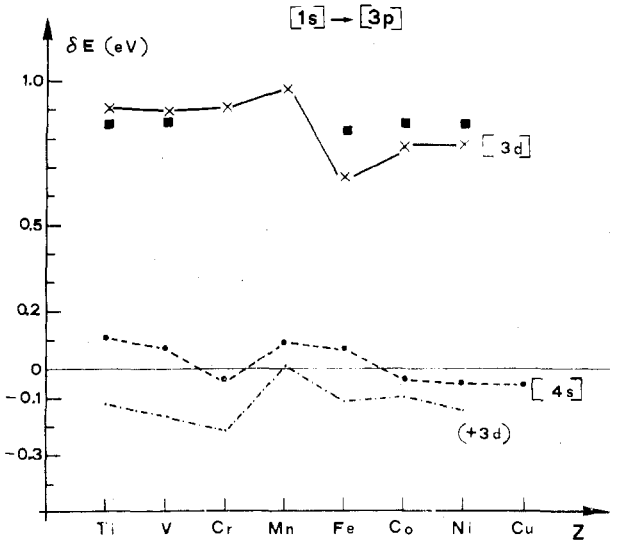

Figure 3. Same as Figure 2 for $K\beta_{1,3}$ fluorescence lines. The legend for each curve is also the same.

density of the d functions is larger around 2p orbitals than around 1s orbitals; hence there will be larger interactions with the 2p "tails" than with the 1s ones.[26,27]

When inner electrons have larger principal quantum numbers, viz., 3s and 3p orbitals, such a local, effective potential picture is no longer valid with respect to 3d interaction[24] and therefore the relevant radiative decay processes will exhibit positive shifts in eq 8 since for the final states involved the 3d screening appears to be much less effective than for the K-shell electrons which still follow the coulombic model.

The general behavior of such effects as a function of the atomic number Z is pictorially reported in Figures 2–5 for negative and positive ions and for all the relevant fluorescence lines. It is evident from such figures that, within the small oscillations generated by configuration differences, the expected shifts follow the same trend along the series and that for transition metals the interplay between 4s and 3d behavior could provide a useful tool for estimating *total* shifts from compounds in different chemical oxidation states.

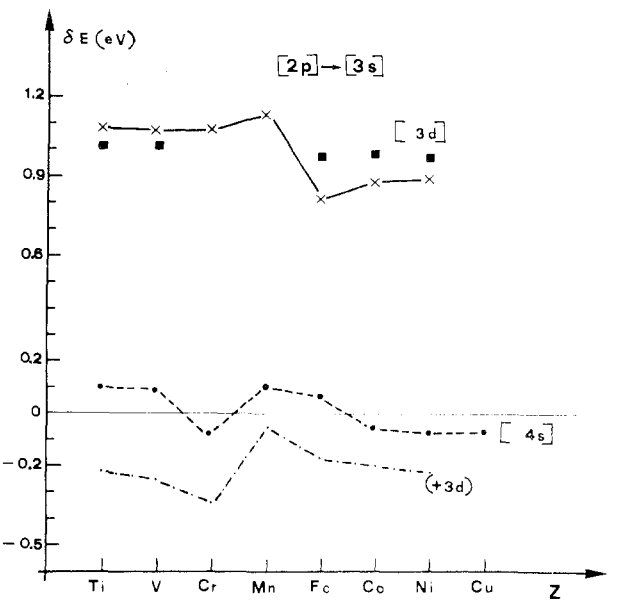

Figure 4. Same as Figure 3 for $L_{II}M_I$ fluorescence lines.

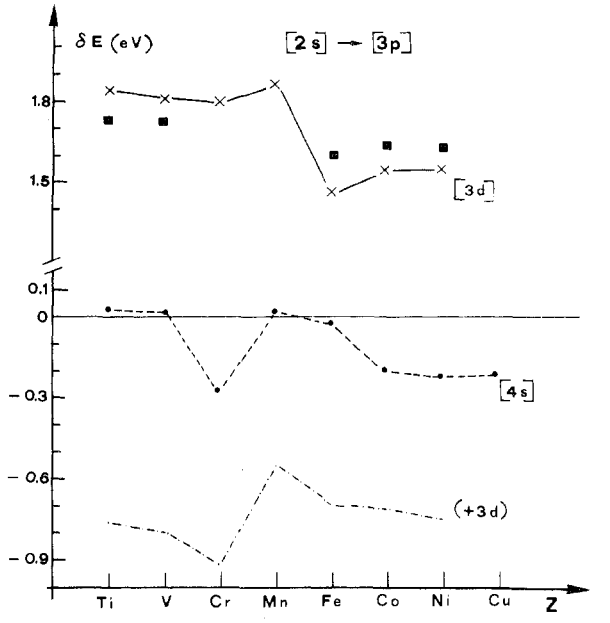

Figure 5. Same as Figure 4 for $L_IM_{II,III}$ fluorescence lines.

This, however, should be done with great care and only for those fluorescence decays for which the "free-ion" model, hence the local interactions, can provide realistic, albeit simplified, descriptions for the charge reorganization following bond formation.

Registry No. Ti, 7440-32-6; V, 7440-62-2; Cr, 7440-47-3; Mn, 7439-96-5; Fe, 7439-89-6; Co, 7440-48-4; Ni, 7440-02-0; Cu, 7440-50-8; Ti^+, 14067-04-0; V^+, 14782-33-3; Cr^+, 14067-03-9; Mn^+, 14127-69-6; Fe^+, 14067-02-8; Co^+, 16610-75-6; Ni^+, 14903-34-5; Cu^+, 17493-86-6; Ti^-, 22325-58-2; V^-, 16727-17-6; Cr^-, 19498-56-7; Mn^-, 22325-60-6; Fe^-, 22325-61-7; Co^-, 16727-18-7; Ni^-, 33383-01-6; Ti^{2+}, 15969-58-1; V^{2+}, 15121-26-3; V^{3+}, 22541-77-1.

References and Notes

(1) See, for instance, D. A. Shirley, Ed., *Electron Spectrosc., Proc. Int. Conf.*, 471 (1972).
(2) L. Hedin and A. Johansson, *J. Phys. B*, **2**, 1336 (1969).
(3) F. A. Gianturco et al., *Chem. Phys. Lett.*, **30**, 235 (1975).

(4) T. A. Carlson, *Phys. Electron. At. Collisions, Invited Lect. Prog. Rep. Int. Conf.*, **8**, 205 (1973).
(5) F. A. Gianturco and C. A. Coulson, *Mol. Phys.*, **14**, 223 (1968).
(6) T. A. Carlson and M. O. Krause, *Phys. Rev.* [*Sect.*] *A*, **140**, 1057 (1965).
(7) R. McWeeny and B. T. Sutcliffe, "Methods of Molecular Quantum Mechanics", Academic Press, London, 1969.
(8) D. A. Shirley, *Adv. Chem. Phys.*, **23**, 85 (1973).
(9) I. Oksuz and O. Sinanoglu, *Phys. Rev.*, **181**, 42 (1969).
(10) R. Fässler and P. Mecke, *Z. Elektrochem.*, **64**, 587 (1960).
(11) C. A. Coulson and C. Zauli, *Mol. Phys.*, **6**, 525 (1963).
(12) F. A. Gianturco and C. A. Coulson, *Inorg. Chim. Acta*, **3**, 607 (1969).
(13) J. A. Bearden and A. F. Burr, *Rev. Mod. Phys.*, **39**, 78 (1967).
(14) M. Bossa, F. A. Gianturco, and F. Maraschini, *J. Electron Spectrosc. Relat Phenom.*, **6**, 27 (1975).
(15) A. Rosen and I. Lindgren, *Phys. Rev.*, **176**, 114 (1968).
(16) F. A. Gianturco, E. Semprini, and F. Stefani, submitted for publication.
(17) E. Clementi and C. Roetti, *At. Data Nucl. Data Tables*, **14**, 177 (1974).
(18) F. A. Cotton and G. Wilkinson, "Advanced Inorganic Chemistry", Interscience, New York, N.Y., 1972.
(19) A. D. Baker and D. Betteridge, "Photoelectron Spectroscopy", Pergamon Press, Oxford, 1972.
(20) K. Siegbahn et al., "ESCA Applied to Free Molecules", North-Holland Publishing Co., Amsterdam, 1972.
(21) D. P. Craig and T. Thirunamachandran, *J. Chem. Phys.*, **45**, 3355 (1966).
(22) G. Leonhardt and A. Meisel, *J. Chem. Phys.*, **52**, 6189 (1970).
(23) P. S. Bagus, *Phys. Rev.*, **118**, 1036 (1965).
(24) P. Politzer and K. C. Daiker, *Chem. Phys. Lett.*, **20**, 309 (1973).
(25) D. T. Clark and D. M. T. Lilley, *Chem. Phys. Lett.*, **9**, 234 (1971).
(26) F. A. Gianturco, *J. Chem. Soc. A*, 23 (1969).
(27) A. Meisel and G. Leonhardt, *Z. Anorg. Allg. Chem.*, **339**, 1 (1965).

Contribution from the Metcalf Research Laboratories,
Brown University, Providence, Rhode Island 02912

Nature of Vanadium(IV) in Basic Aqueous Solution[1]

MELANIE M. IANNUZZI and PHILIP H. RIEGER*

Received May 21, 1975 AIC50356D

Strongly basic aqueous solutions of vanadium(IV) were studied by means of ESR, optical, and Raman spectroscopy. ESR spectra and pH titrations show that vanadium(IV) is monomeric with stoichiometry $VO(OH)_3^-$. Higher oligomers, if present at all, are of minor importance. A strong Raman absorption at 987 cm^{-1} confirms the presence of the vanadyl group in solution. ESR parameters for $VO(OH)_3^-$ are $\langle g \rangle = 1.970$, $\langle a \rangle = -96.1$ G, $g_\parallel - g_\perp = -0.020$, and $a_\parallel - a_\perp = -120$ G. The isotropic hyperfine splitting, unlike that of the aquovanadyl ion, is temperature independent. Electronic transitions were found at 12.8, 19.2, and 24.4 $\times 10^3$ cm^{-1}. Comparison of the spectral data for $VO(OH)_3^-$ with those of $VO(H_2O)_5^{2+}$ suggests that the hydroxo complex is structurally related to the aquo ion by the ionization of three water protons and that the metal-to-ligand σ bonds are somewhat more covalent in $VO(OH)_3^-$ than in $VO(H_2O)_5^{2+}$.

Introduction

The chemistry of vanadium(IV) in acid solutions or in the presence of strongly coordinating ligands is reasonably well understood.[2] The nature of the 4+ state in neutral or basic solutions, on the other hand, has received relatively little study by modern techniques. The interest in oxo anions of vanadium(IV) began with Berzelius,[3] who isolated an oligomeric vanadate(IV) salt. Later analyses of salts from strongly basic solutions of vanadium(IV) by Crow[4] and by Koppel and Goldman[5] led to the formulation $M_2V_4O_9 \cdot xH_2O$ where M is Na, K, NH_4, or Ba/2. Crow[4] also claimed to have obtained $M_2V_2O_5 \cdot xH_2O$ where M is Ag or Pb/2.

Titration curves obtained by Britton[6] and by Ostrowetsky[7] were found to be consistent with the presence of the $V_4O_9^{2-}$ species in basic solution. Ostrowetsky[7] also examined the uv spectrum and found the shape of the charge-transfer band at ca. 325 nm to depend on base concentration in the pH range 13–14. Polarographic studies by three different groups[7-9] were inconclusive and apparently contradictory.

Although there was little reason to doubt the existence of an oligomeric vanadate(IV) in solution when we began our work, there was reason to expect that the description of the system was incomplete. Virtually all other amphoteric oxides are converted to monomeric anions in sufficiently strongly basic media.[10] That VO_2 does not behave similarly would at least be worth verifying. Thus the goal of this work was to characterize the species found in basic solutions of vanadium(IV) and to elucidate the equilibria connecting them. Only one species was found—a monomer—and no evidence was obtained for polymeric oxo anions in solution above pH 12.

Experimental Section

Acidic stock solutions of vanadyl perchlorate were prepared from Fisher vanadyl sulfate and analyzed by permanganate titration as described earlier.[11] Basic solutions of vanadium(IV) were prepared by rapid addition of the vanadyl perchlorate solution to a solution of sodium hydroxide with vigorous stirring under positive nitrogen pressure in a gastight cell. Nitrogen gas was bubbled through both solutions for about 30 min before mixing to remove dissolved oxygen.

pH titrations were carried out in a gastight titration vessel under nitrogen using a Coleman 30 pH meter and a Coleman 3-265 combination electrode, calibrated with Fisher BuffAR standards at pH 4.0 and 7.0. The titrant—NaOH or $HClO_4$ solutions—was added in 0.1-ml increments with a Hamilton syringe pipet.

X-Band ESR spectra were obtained with a Varian V-4502 spectrometer using 100-kHz field modulation. Spectra were obtained at ambient temperature with samples contained in a Varian aqueous sample cell which was part of a closed-loop flow system which included the titration vessel. This system allowed samples to be introduced into the spectrometer cavity without changing the position of the sample cell or exposing the sample to the atmosphere. At temperatures other than ambient, samples were contained in thin-walled capillaries which were filled in a nitrogen-filled glove bag. Temperature control was with a Varian variable-temperature accessory. The magnetic field was calibrated by proton resonance, and the microwave frequency was determined by observation of the electron resonance of a DPPH sample ($g = 2.0036$[12]) taped to the sample tube.

Optical spectra were recorded on a Cary 14 spectrophotometer using the closed-loop flow system including the titration vessel and a 10-cm absorption cell. Spectra were obtained in the 220–1000-nm range for basic solutions of vanadium(IV) varying in concentration from 0.12 to 1.5 m*M*.

Raman spectra of 5.0 m*M* solutions of vanadium(IV) in 1.0 *M* NaOH were obtained with a Jarrell-Ash 25-300 Raman spectrograph operating with laser excitation at 514.5 nm and covering the range 900–2000 cm^{-1}. Samples were prepared in a nitrogen-filled glove bag and transferred to a multiple reflectance cell for observation of the spectrum.

Results and Discussion

Stoichiometry of the Reaction of the Vanadyl Ion with Base. Titration of a 5 m*M* solution of $VO(ClO_4)_2$ in 1.0 *M* $NaClO_4$ with 1.00 *M* NaOH proceeded with precipitation of a gray solid—presumably hydrated VO_2—starting about pH 4. The precipitate increased in quantity until a clear colorless su-